Supporting Information

A Dual-responsive Colorimetric Probe for Detection of Cu^{2+} and Ni^{2+} Species in Real Water Samples and Human Serum

Guoxing Yin,[a] Jingfeng Yao,[a] Sai Hong,[a] Yinuo Zhang,[a] Zhaohua Xiao,[b] Ting Yu,[a,*] Haitao Li[a] and Peng Yin[a,*]

[a] Key Laboratory of Chemical Biology and Traditional Chinese Medicine Research (Ministry of Education), College of Chemistry and Chemical Engineering, Hunan Normal University, Changsha 410081, China.

[b] Xiangya Hospital of Central South University, Changsha 410008, China.

Table of Contents

I. Experimental Section

Calculation of the detection limit (LOD)

$$\mathrm{LOD} = 3\sigma/S$$

$$\sigma = \sqrt{\frac{\sum(\bar{x} - x_i)^2}{n-1}}$$

σ: the standard deviation of the blank solution.

$\bar{x}$ is the mean of the blank measures; x_i is the values of blank measures; n is the number of tested blank measure (n = 10)

S: the slope of the linear calibration plot between the absorption intensity and the concentration of Cu^{2+} or Ni^{2+}.

II. Supplementary Spectra

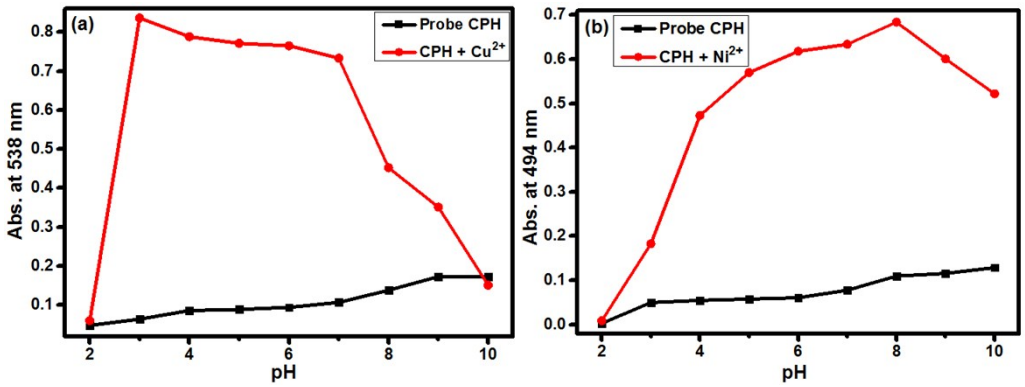

Fig. S1 (a) Profile of pH dependence of the absorption intensity of probe CPH (10 μM) at 538 nm in the absence and presence of 2.0 equiv. of Cu^{2+} in water. (b) Profile of pH dependence of the absorption intensity of probe CPH (10 μM) at 494 nm in the absence and presence of 1.0 equiv. of Ni^{2+} in water. The pH of water is 2, 3, 4, 5, 6, 7, 8, 9 and 10.

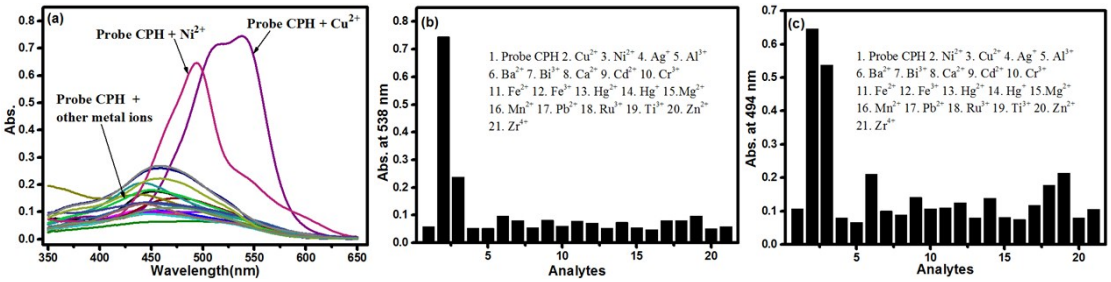

Fig. S2 (a) Absorption intensity spectra of probe CPH (10 μM) upon addition of 10 eq. (100 μM) of various metal ions in pure water at room temperature. (b) Histogram representing the absorption intensity at 538 nm, (c) Histogram representing the absorption intensity at 494 nm. Each spectrum was recorded after addition of the corresponding species and shaked well. Metal ions: Cu^{2+}, Ni^{2+}, Ag^{+}, Bi^{3+}, Zr^{4+}, Fe^{2+}, Cd^{2+}, Pb^{2+}, Fe^{3+}, Ba^{2+}, Mg^{2+}, Mn^{2+}, Zn^{2+}, Hg^{2+}, Ca^{2+}, Cr^{3+}, Ru^{3+}, Hg^{+}, Ti^{3+} and Al^{3+}.

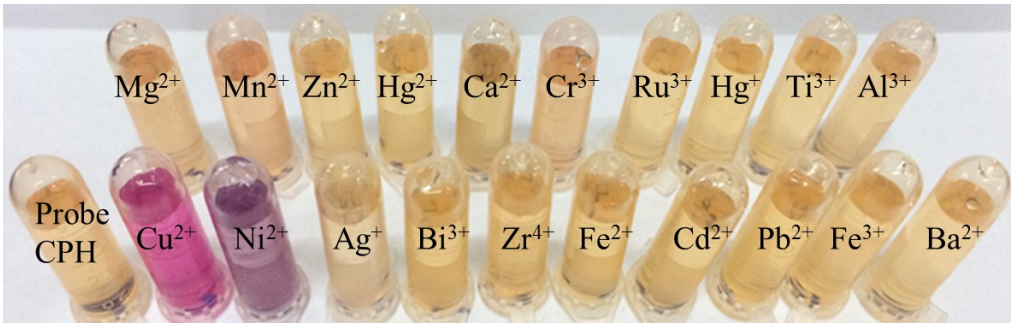

Fig. S3 The photograph of probe CPH (10 μM) in the presence of various metal ions (10.0 equiv.) including probe CPH alone, Cu^{2+}, Ni^{2+}, Ag^{+}, Bi^{3+}, Zr^{4+}, Fe^{2+}, Cd^{2+}, Pb^{2+}, Fe^{3+}, Ba^{2+}, Mg^{2+}, Mn^{2+}, Zn^{2+}, Hg^{2+}, Ca^{2+}, Cr^{3+}, Ru^{3+}, Hg^{+}, Ti^{3+} and Al^{3+} in pure water at room temperature.

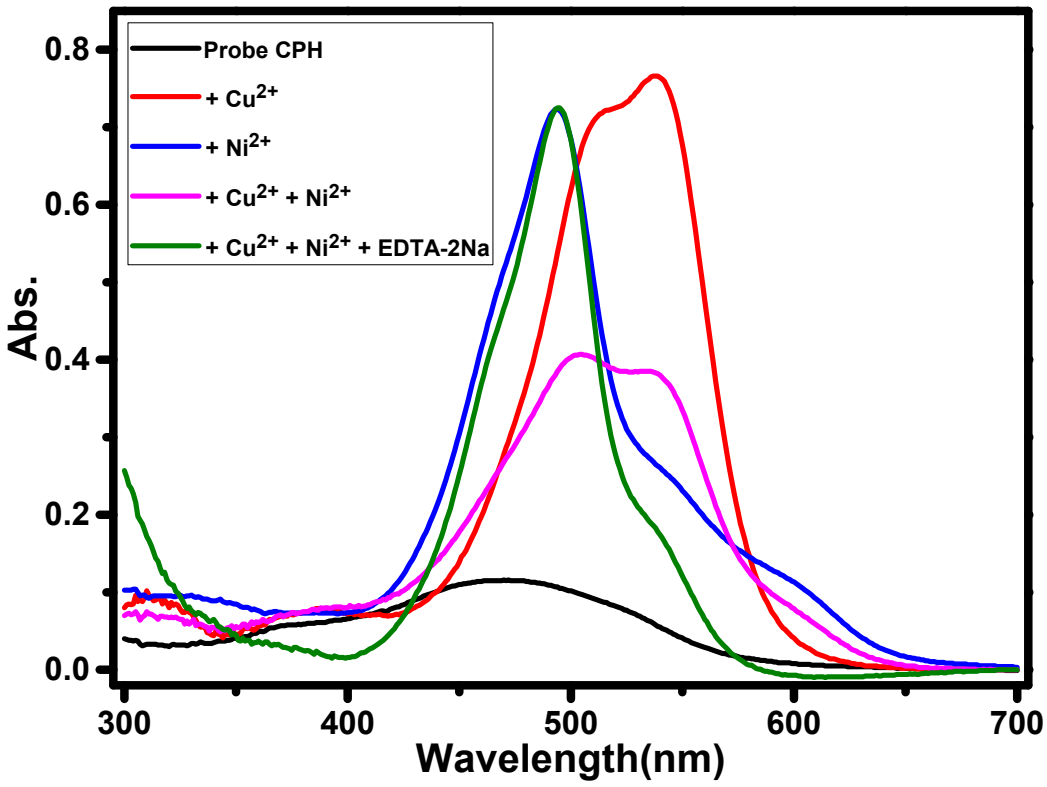

Fig. S4 Absorption spectra of probe CPH (10 μM) in the presence of various analysts. Black line (CPH, 10 μM), red line (CPH (10 μM) + Cu^{2+} (10 μM)), blue line (CPH (10 μM) + Ni^{2+} (10 μM)), pink line (CPH (10 μM) + Cu^{2+} (10 μM) + Ni^{2+} (10 μM)), green line (CPH (10 μM) + Cu^{2+} (10 μM) + Ni^{2+} (10 μM) + EDTA-2Na (100 μM)).

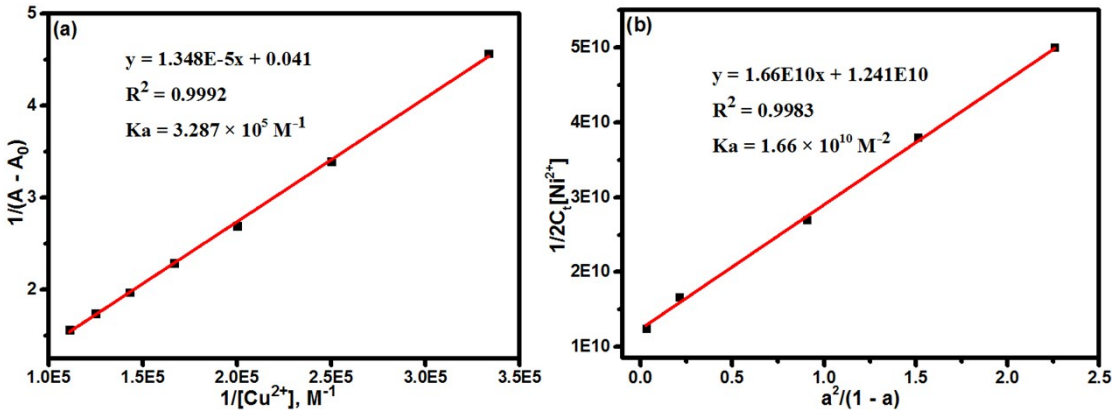

Fig. S5 (a) Benesi-Hildebrand plot (absorbance at 538 nm) of CPH with Cu^{2+}. From the plot, we could obtain the association constants (K_a) of CPH with Cu^{2+} is 3.287 × 10^5 M^{-1}. (b) Li's equation plot (absorbance at 494 nm) of CPH, assuming 2:1 stoichiometry for association between CPH and Ni^{2+}. 'Ct' means the concentration of CPH, and 'a' does $[(A_x-A_{max})/(A_0-A_{max})]$. The association constants (K_a) of CPH with Ni^{2+} is 1.66 × 10^{10} M^{-2}.

Note: The association constant (K_a) of CPH with Cu^{2+} was determined based on the absorbance titration curve using the Benesi-Hildebrand equation as follows:

$1/(A_{max} - A_0) = [1/(A - A_0)]\times[1/(K_a \times [Cu^{2+}]+ 1)]$

where A and A_0 represent the absorbance of host in the presence and absence of ions, respectively, A_{max} is the saturated absorbance of host in the presence of excess amount of ions; $[Cu^{2+}]$ is the concentration of Cu^{2+}added.

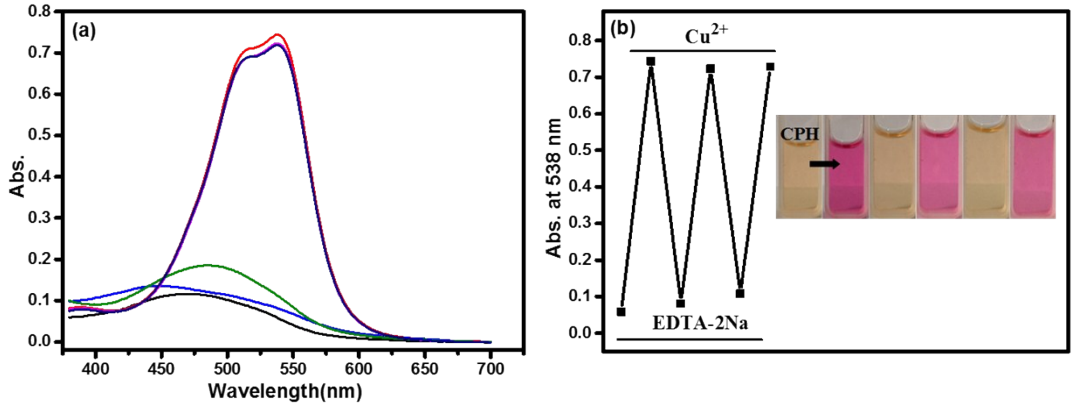

Fig. S6 (a) Change of absorption spectra of CPH after alternate addition of Cu^{2+} and EDTA-2Na. Black line (CPH), red line (CPH + Cu^{2+}), blue line (CPH + Cu^{2+} + EDTA-2Na), purple line (CPH + Cu^{2+} + EDTA-2Na + Cu^{2+}), green line (CPH + Cu^{2+} + EDTA-2Na + Cu^{2+} + EDTA-2Na), pink line (CPH + Cu^{2+} + EDTA-2Na + Cu^{2+} + EDTA-2Na + Cu^{2+}) and (b) reversibility studies. The inset photos show the visible-light color changes of probe CPH (10 μM) under different conditions. Each spectrum was recorded after addition of the Cu^{2+} / EDTA-2Na and shaked well.

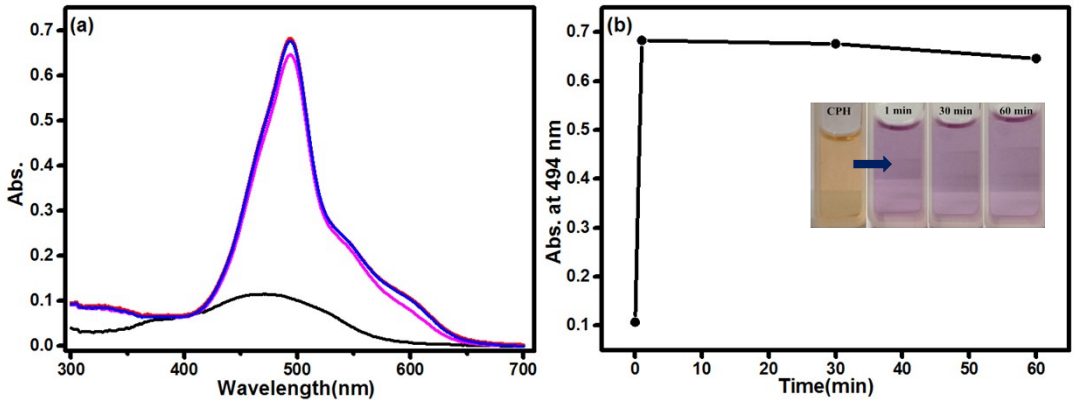

Fig. S7 (a) Changes of absorption spectra of CPH after the addition of Ni^{2+} and citric acid. Black line (CPH), red line (CPH + Ni^{2+}) for 1 min, blue line (CPH + Ni^{2+} + citric acid) for 30 min, pink line (CPH + Ni^{2+} + citric acid) for 60 min at room temperature. (b) The absorption intensity at 494 nm at different time. The inset photos show the visible-light color changes of probe CPH (10 μM) and CPH (10 μM) upon addition 10 equiv. of Ni^{2+} and 100 equiv. of citric acid under visible light at different time.

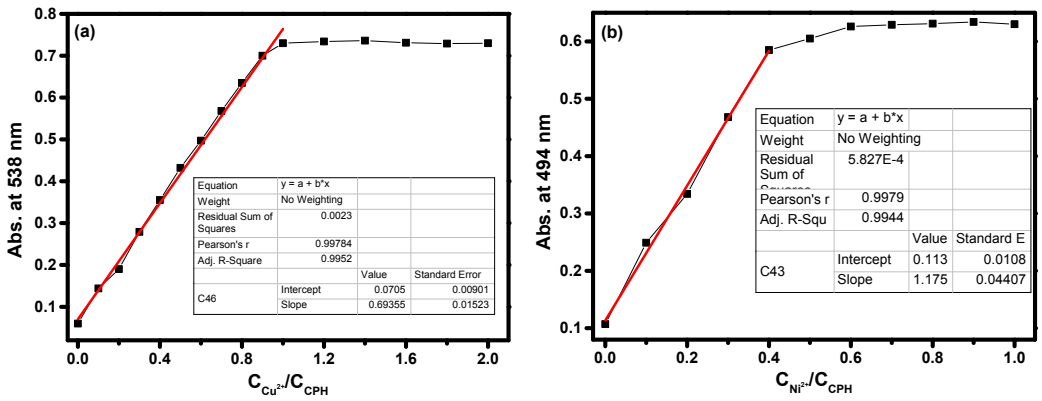

Fig. S8 The linear changes of the absorption intensities of probe CPH at (a) 538 nm and (b) 494 nm and as a function of Cu^{2+}/Ni^{2+} concentration.

III. ^{1}H NMR, ^{13}C NMR and HRMS chart

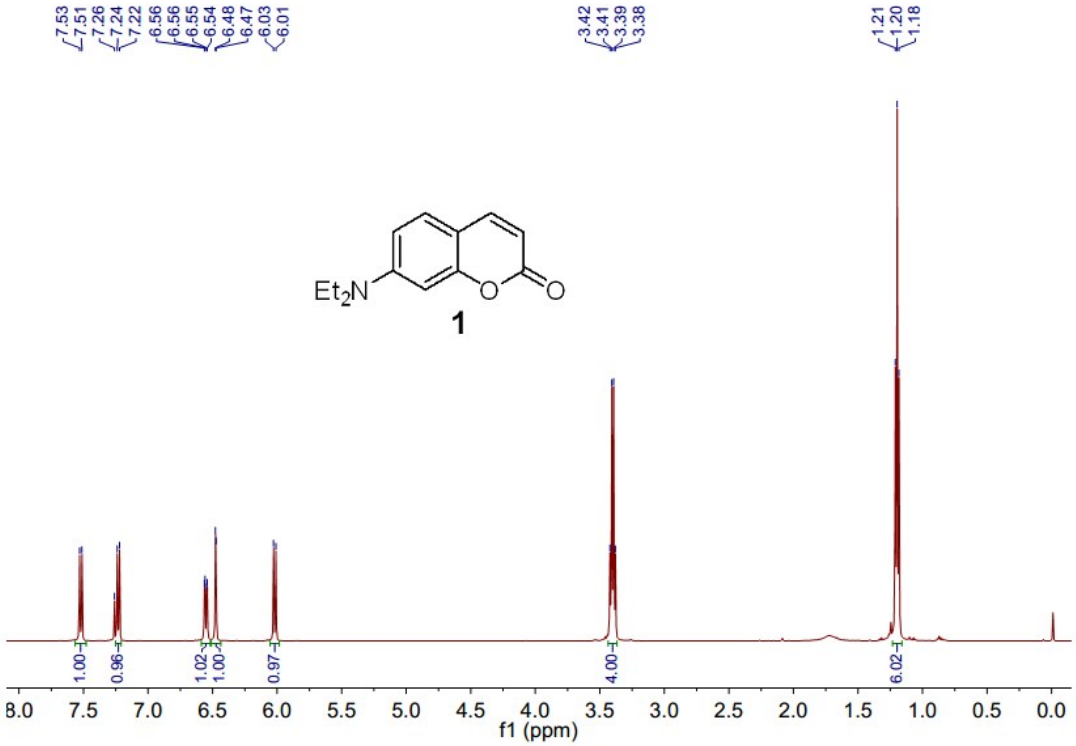

Fig. S9 ^{1}H NMR spectrum of compound **1** in $CDCl_3$.

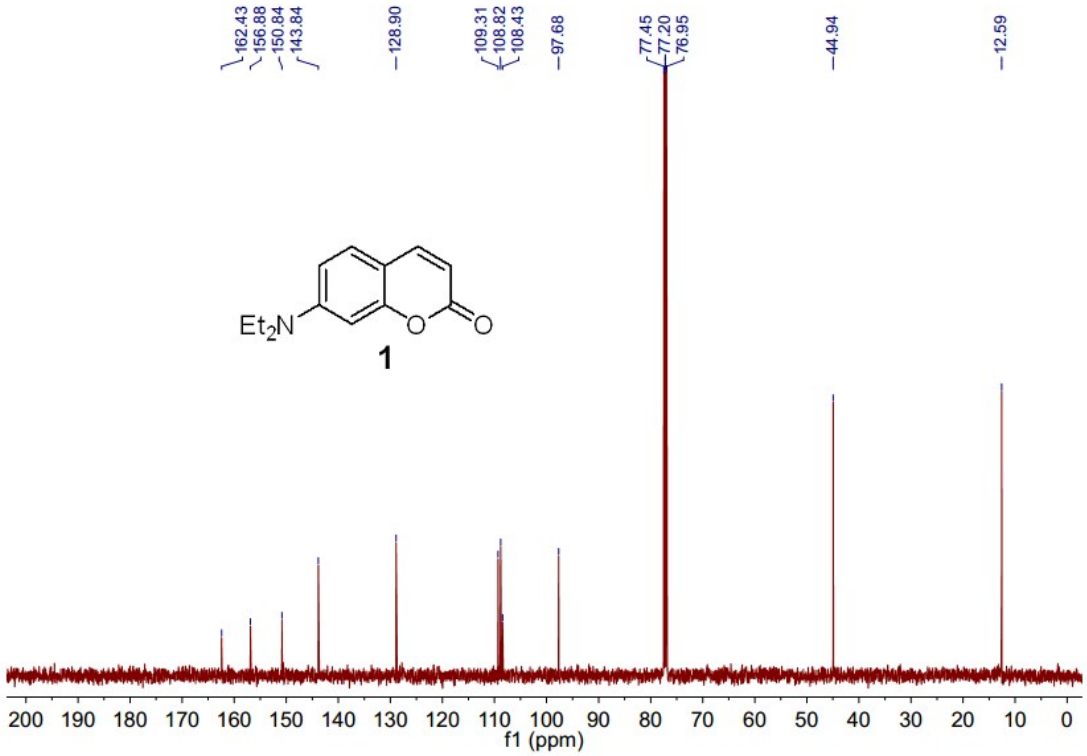

Fig. S10 ^{13}C NMR spectrum of compound **1** in $CDCl_3$.

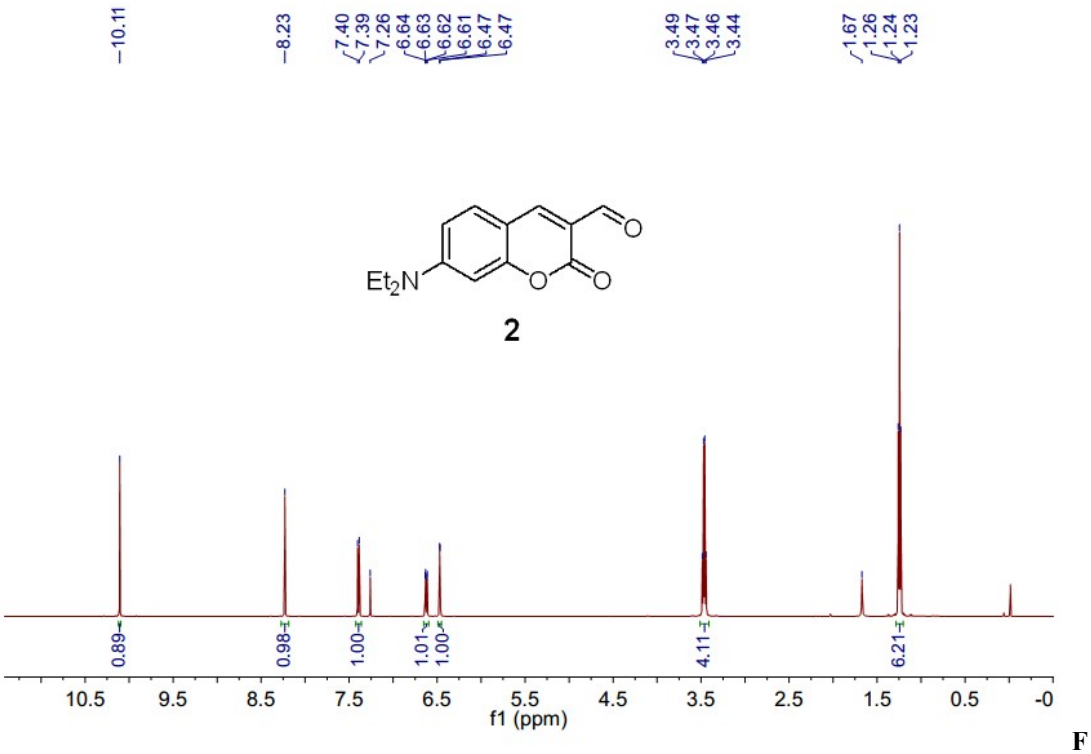

F

ig. S11 ^{1}H NMR spectrum of compound **2** in $CDCl_3$.

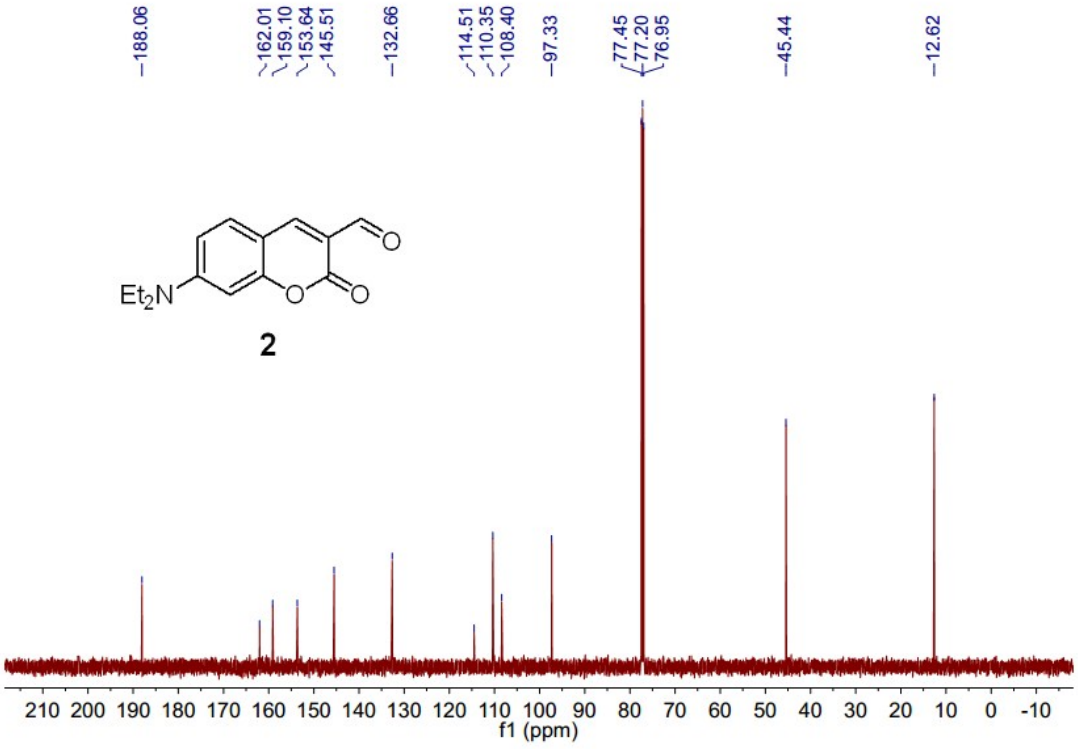

Fig. S12 ^{13}C NMR spectrum of compound **2** in $CDCl_3$.

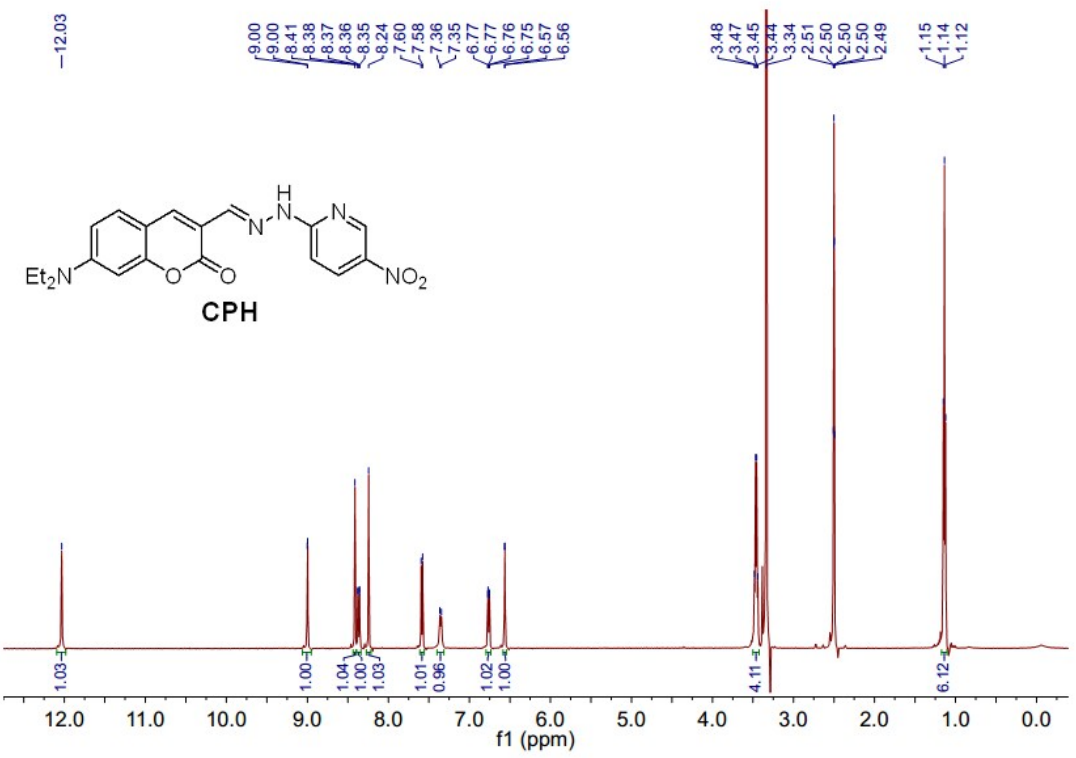

Fig. S13 ^{1}H NMR spectrum of probe CPH in DMSO-d_6.

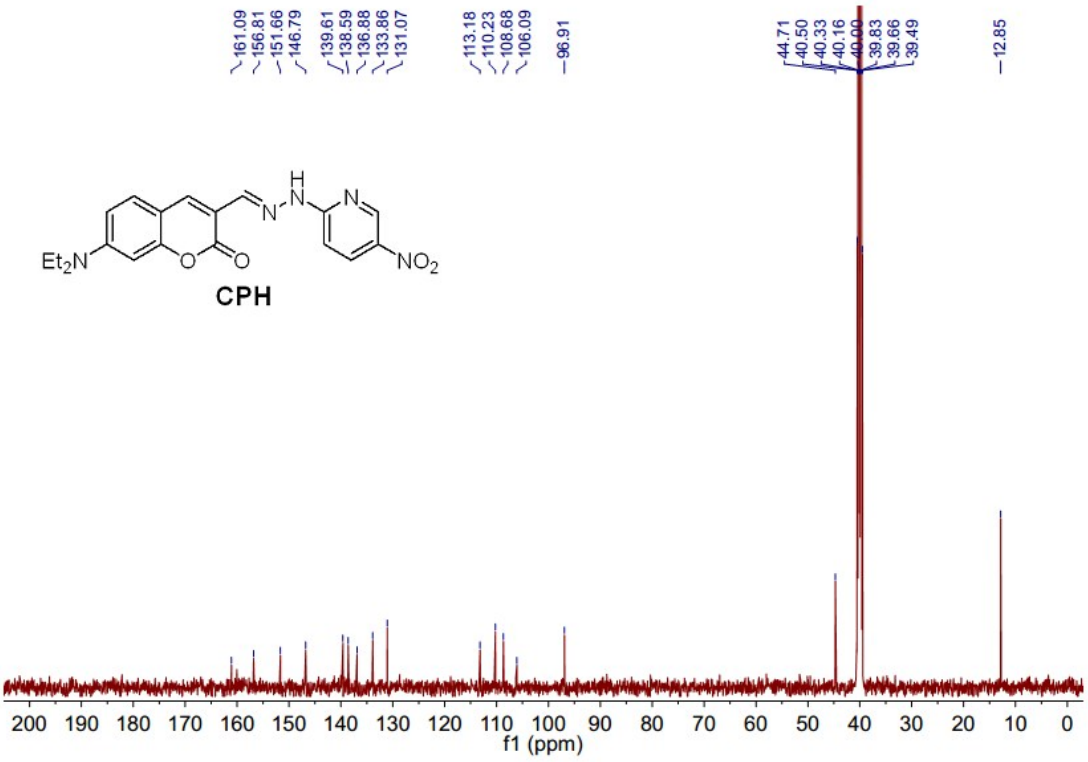

Fig. S14 ^{13}C NMR spectrum of probe CPH in DMSO-d_6.

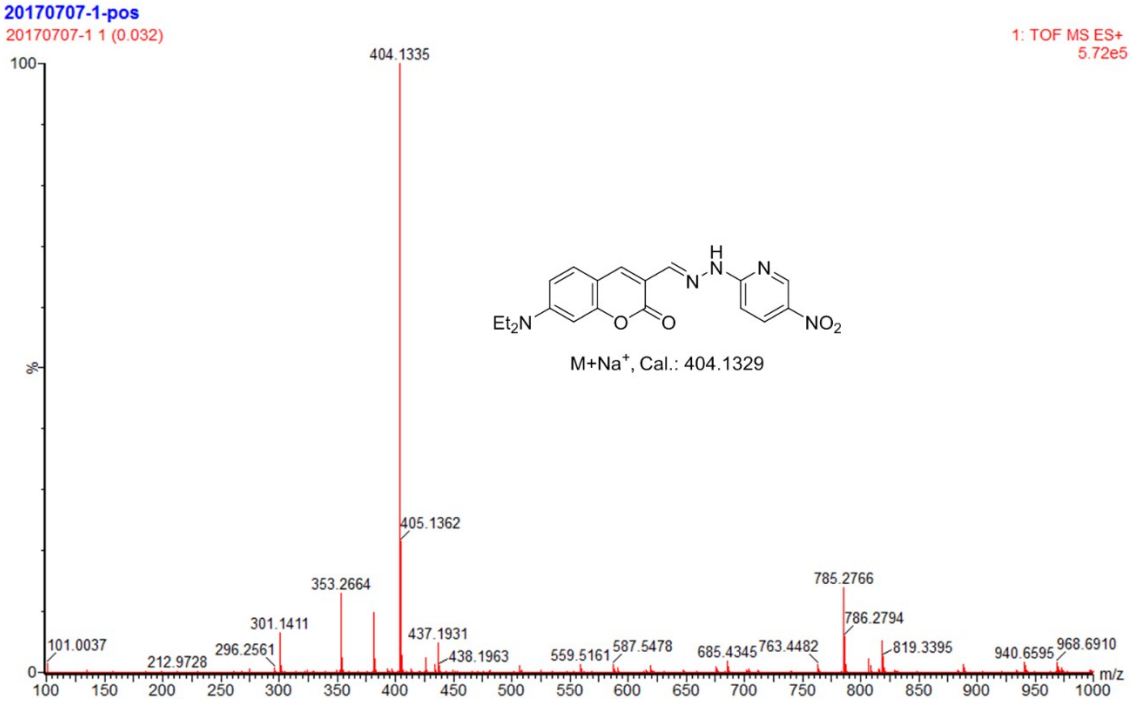

Fig. S15 HRMS spectrum of probe CPH.

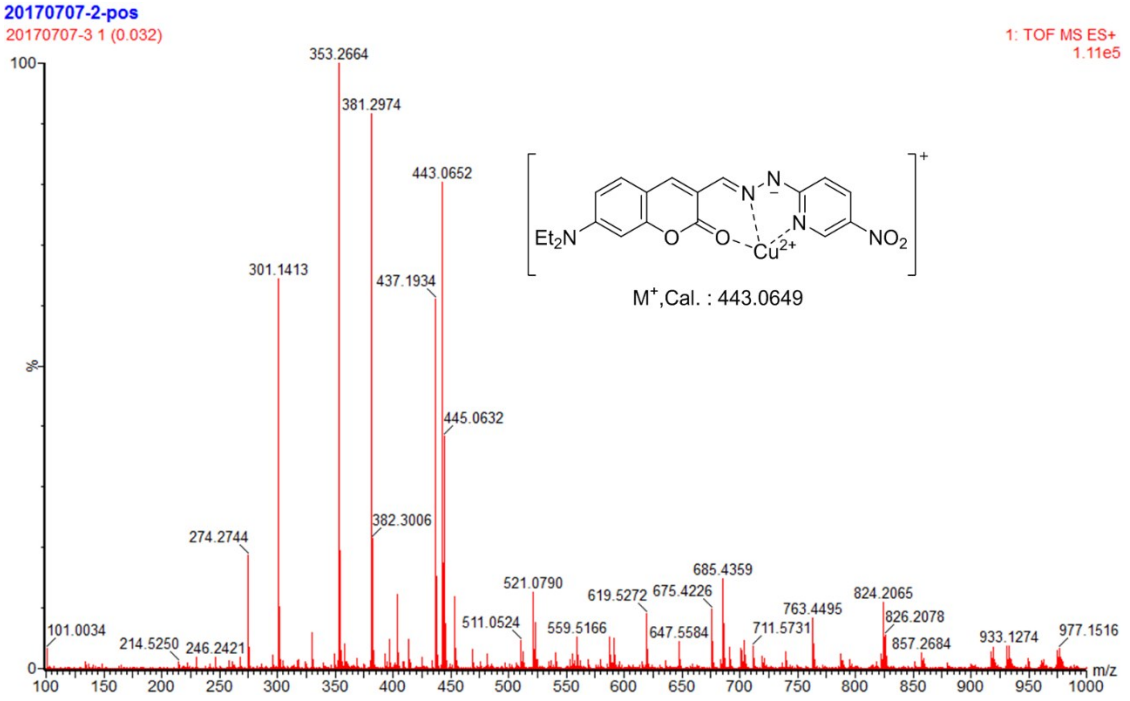

Fig. S16 HRMS spectrum of the product from the reaction between probe CPH and $CuSO_4$.

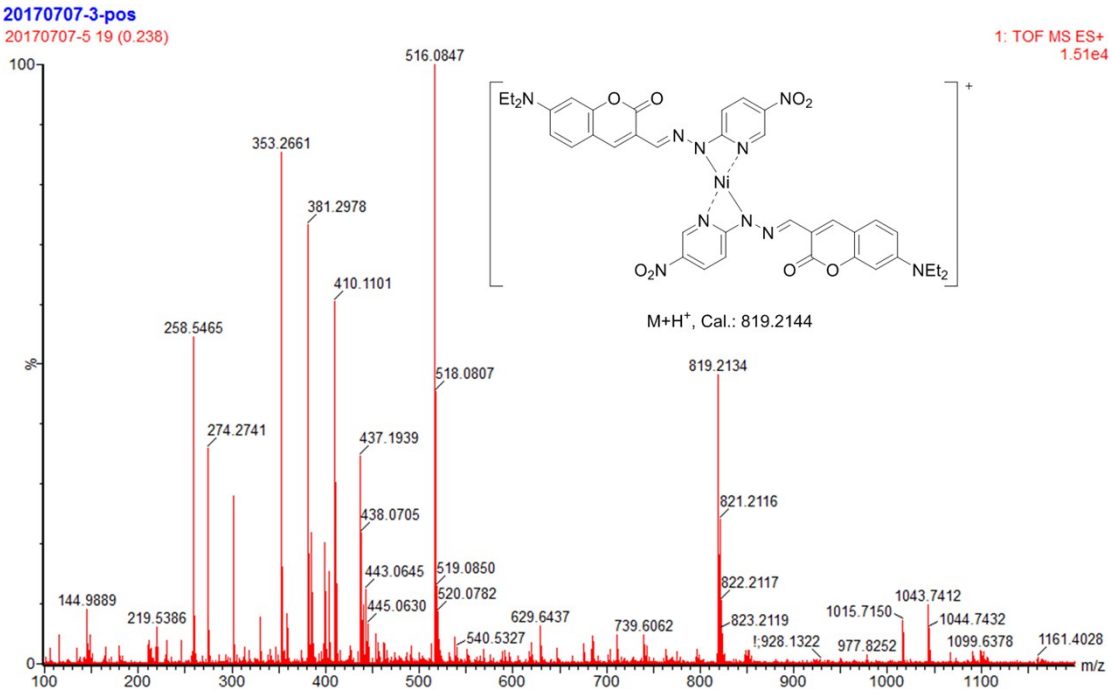

Fig. S17 HRMS spectrum of the product from the reaction between probe CPH and $NiSO_4$.